ACS OMEGA

Open Access

http://pubs.acs.org/journal/acsodf

Article

Taif Rose Oil Ameliorates UVB-Induced Oxidative Damage and Skin Photoaging in Rats via Modulation of MAPK and MMP Signaling Pathways

Published as part of the ACS Omega virtual special issue "Phytochemistry".

Hossam M. Abdallah,* Abdulrahman E. Koshak, Mohamed A. Farag, Nesrine S. El Sayed, Shaimaa M. Badr-Eldin, Osama A. A. Ahmed, Mardi M. Algandaby, Ashraf B. Abdel-Naim, Sabrin R. M. Ibrahim, Gamal A. Mohamed, Peter Proksch, and Haidy Abbas

Cite This: *ACS Omega* 2023, 8, 33943−33954

Read Online

ACCESS | Metrics & More | Article Recommendations | Supporting Information

ABSTRACT: Short-wave UVB (ultraviolet B) causes rapid oxidative damage to the skin. Rose water is obtained mainly from the petals of *Rosa damascena* Mill. (Rosaceae) and used traditionally to hydrate dry skin and reduce signs of aging. This work aimed at evaluating the possible protective potential of the prepared eco-friendly Taif rose oil nanoemulsion (ROSE-NANO) against UVB-induced photoaging in adult male Wistar rats. Taif rose oil (ROSE) was obtained from *R. damascene* by classical steam distillation and formulated in emulgel (100 mg/g). In addition, the oil was formulated in ROSE-NANO-loaded emulgel (50 and 100 mg/g) to enhance the effect of ROSE. All prepared formulas were tested topically for their potential protective effect in UV-induced skin photoaging. The obtained results demonstrated that application of ROSE-NANO-loaded emulgel resulted in superior antiaging potency over ROSE emulgel based on histological studies as well as biochemical evaluations via amendment in CAT and SOD activities, decreasing the concentration of the inflammatory markers and preventing collagen fragmentation through reduction of MMP-9 content in fibroblasts. Moreover, a significant decrease in mRNA expression of NF-KB, JNK, ERK1/2, and p38 MAPK genes was observed. In conclusion, the current study provides scientific evidence for the traditional use of rose oil in skin aging. Moreover, the NANO formula showed promising efficacy as a skin photoprotector against UV-induced oxidative damage and skin aging.

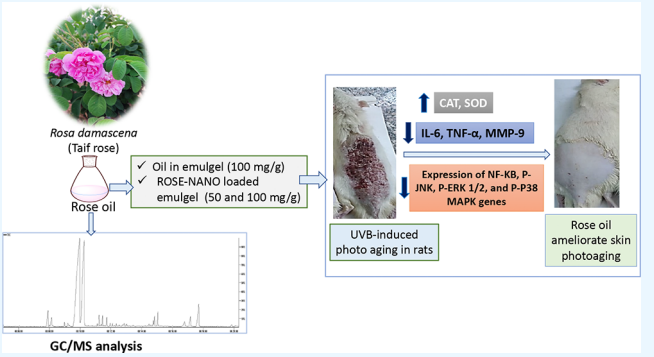

1. INTRODUCTION

Family Rosaceae includes 200 species and more than 18,000 cultivars, of which *Rosa damascena* is the most famous and important.[1] Rose oil is obtained mainly from the petals of *R. damascena* (Rosaceae), which is also known as damask rose, since it was brought from Damascus to Europe.[2]

The plant is well known not only for its medicinal and pharmacological effects but also because of its holy beliefs. In Iran, this flower is known as Gol-E-Muhammadi (the flower of Muhammad).[3] Nevertheless, most commercial rose oil is derived from *R. damascena*, including Bulgarian and Turkish rose essential oils, which are the world's major producers.[2] West Saudi Arabian societies have embraced roses as a cultural symbol. *Rosa damascena* Miller var. *trigintipetala* is cultivated on a large scale in Taif governorate, where it is named "Ward Taifi" and is considered one of the industrial crops in this region. Production of rose oil in Saudi Arabia amounted to 5% of the global rose oil production.[4]

The oil is used in cosmetic manufacturers (e.g., body lotions, soaps, face creams) for its fragrance. Meanwhile, it is usually added as a flavoring agent in food manufacturing.[5] Traditionally, a decoction of the flower is used in Iranian medicine for chest and abdominal pains, menstrual bleeding, and digestive ailments and as cardiotonic. Besides being used for cleaning eyes and mouths, it was traditionally used as an antiseptic for alleviating abdominal pain, lung congestion, and bronchial problems.[6] The Damask rose was first described over a thousand years ago by Avicenna (980−1037 AD). It has various medical benefits, including its gastrointestinal and cardiac tonic effects, cosmetic

Received: July 3, 2023
Accepted: August 21, 2023
Published: September 7, 2023

properties that eliminate sweat odor, skin, and mucosal repair, antinociceptive properties, and anti-inflammatory effects. Rose water is used traditionally to hydrate dry skin, reduce signs of aging, and strengthen facial skin.[7]

Modern medicine has proven its different pharmacological activities including hypnotic, antimicrobial, anticonvulsant, analgesic, antidiabetic, anti-inflammatory, anti-HIV, and antioxidant.[2] Further, due to its antibacterial effect, the oil is used in treating acne.[2] Moreover, consuming *R. damascena* as functional food induces a protective effect in skin aging induced by ultraviolet through collagen synthesis enhancement as well as increased expression of TGF-b1.[8]

The exposure of skin to UV radiation can produce reactive oxygen species (ROS), which lead to oxidative damage and accumulation of oxidative products, both of which are indicators of oxidative stress in the tissue causing skin aging.[9] Moreover, UV irradiation of the skin causes the expression of elastase and collagenase, leading to wrinkles and sunburn on the skin.[10] As a result, unprotected UVB exposure is a recognized factor in the onset of early aging symptoms.[11] The skin's vulnerability to oxidative stress and ROS production are the primary indicators of early photoaging.[12] Additionally, UV light causes the skin to have acute inflammatory reactions that speed up the aging process.[13] Previously, it was known that topical application of antioxidants protects skin from oxidative damage.[14] Several natural antioxidant ingredients also have anti-inflammatory properties that can be used in the treatment of oxidative damage-associated conditions such as photoaging.[15] In this work, ROSE emulgel (100 mg/g) as well as an eco-friendly Taif rose oil nanoemulsion (ROSE-NANO) was prepared at two dose levels (50 and 100 mg/g emulgel) to study their possible protective effect against UVB-induced photoaging. Its protective effect was assessed by measuring antioxidant parameters: SOD and CAT; anti-inflammation markers: TNF-α and IL-6; and antiwrinkle parameter: MMP-9. Additionally, total RNA isolated from rat dissected joints was used to analyze the expression of JNK, ERK1/2, and p38 MAPK genes.

2. EXPERIMENTAL SECTION

2.1. Chemicals and Reagents. α-Cyclodextrin (MW = 972 Da) was procured from Merck Life Science (Darmstadt, Germany). TNF-α (tumor-necrosis factor-α), SOD (superoxide dismutase), and MMP-9 (matrix metalloproteinases 9) were measured employing an ELISA kit following the stated guidance (Glory Science Co, Ltd.). A CAT (catalase) enzyme-linked immunosorbent assay ELISA kit and IL-6 (interleukin 6) were acquired from MyBioSource, Inc. (San Diego/CA) and CUSABIO Inc. (Wuhan/Hubei/China), respectively.

2.2. Preparation of Rose Oil (ROSE). A volatile oil was prepared from the petals of *R. damascena* Miller var. *trigintipetala* (Taif rose) by the classical hydrodistillation method under the supervision of the corresponding author from one of the Taif rose factories (Taif governorate, Saudi Arabia). The collected oil was dried over anhydrous sodium sulfate, filtered, and kept at −20 °C for experimental studies.

2.3. Essential Oil GC/MS Analysis. Three biological replicates of the oil specimen (10 μL) were dissolved in 1 mL of methylene chloride (GC grade) and analyzed by GC-17A gas chromatography (Shimadzu, Tokyo, Japan) coupled with a QP-5000 mass spectrometer (Shimadzu, Tokyo, Japan). The samples were chromatographed on a DB5-MS column (J&W Scientific/Santa Clara/CA) with a length of 30 m, an internal diameter of 0.25 mm, and 0.25 μm film thickness using the splitless mode of injection and helium (a carrier gas) at a 1 mL/min flow rate. The temperature programming was as follows: starting at 38 °C for 3 min, increased temperature to 180 °C with a rate of 12 °C/min, retained for 5 min at 180 °C, increased to 220 °C with a rate of 40 °C/min, and finally kept at 220 °C for 2 min as previously discussed.[16] The peak identity was confirmed by adopting AMDIS software (www.amdis.net), matching the mass spectrum with NIST, as well as its KOVAT index, and comparing it with the standard when available.

2.4. Preparation of an Eco-friendly Rose Oil Nanoemulsion (ROSE-NANO). An eco-friendly rose oil nanoemulsion was prepared using a modified previously reported approach utilizing high shear homogenization.[17,18] ROSE (150 mg), α-cyclodextrin (α-CD, 50 mg), and water (1 g) were homogenized at ambient temperature for 5 min (T25 digital Ultra-Turrax/IKA/Staufen/Germany) at a speed of 15,000 rpm. The prepared ROSE-NANO was kept at 8 °C for biological study.

2.4.1. Droplet Size and Polydispersity Index Determination. The droplet diameter (expressed as *z*-average) was measured after diluting the prepared emulsion with double distillation using the dynamic light scattering technique. In addition, the polydispersity index (PDI) of the developed ROSE-NANO was determined using a Zetasizer Nano ZSP (Malvern Panalytical Ltd./Malvern/U.K.).

2.4.2. Preparation of ROSE-NANO Emulgel. ROSE-NANO emulgel was prepared at two different concentrations (50 and 100 mg/g emulgel). The prepared ROSE-NANO was dispersed in water with hydroxypropyl methylcellulose (HPMC) as a gelling agent and then homogenized at ambient temperature for 2 min at a speed of 10,000 rpm. The prepared dispersion was sonicated for 5 min in a water bath sonicator and then kept in the refrigerator for 24 h. Rose oil-loaded gel (ROSE emulgel) was prepared with the same method at a concentration of 50 mg/g HPMC gel. Also, α-CD-loaded gel (plain NANO-loaded gel) was prepared with the same method and used in the same equivalent concentration used in the 100 mg/g ROSE-NANO emulgel preparation.

2.5. Biological Study. *2.5.1. Animals.* The experiment was performed on the hairless skin of adult male Wistar rats weighing between 180 and 220 g (6−8 weeks old) obtained from the animal house of the National Research Center, Giza, Egypt. The animals were housed in plastic cages and kept in a conditioned atmosphere at 22 ± 3 °C and 50−55% humidity with 12/12 h light/dark cycles. They were fed standard pellet chow (El-Nasr Chemical Company, Cairo, Egypt) and were permitted free access to water. The animals were subjected to one week habituation period before starting the experiment. The experimental procedures were reviewed and approved by the Ethics Committee of the Faculty of Pharmacy, Cairo University (Permit number: PT2949). The study also fulfilled the recommendations of the National Institutes of Health Guide for Care and Use of Laboratory Animals (2011). All efforts were made to minimize the animal distress throughout the experimental period.

2.5.2. Experimental Design. Sixty rats were randomly divided into six groups, each containing 10 animals: group 1: non-UVB-irradiated group, group 2: UVB-irradiated group, group 3: irradiated and topically pretreated with 0.5 g of the plain NANO formulation (vehicle), group 4: irradiated and topically pretreated with 0.5 g of ROSE-loaded gel (100 mg/g), and groups 5 and 6 were irradiated and topically pretreated with 0.5 g

https://doi.org/10.1021/acsomega.3c04756
ACS Omega 2023, 8, 33943−33954

Table 1. Relative Percentage of Detected Volatile Constituents in *R. damascena* Mill. Flowers Using GC/MS Analyses (n = 3)

no.	average Rt(min)	KI	compound name	percentage ± SD
			Alcohols	
1	7.922	954.5	linalool	3.24 ± 0.14
2	8.129	966	phenylethyl alcohol, rose oil	4.96 ± 0.04
3	8.997	1021	1-terpinen-4-ol	0.41 ± 0.05
4	9.25	1031	δ-terpineol	0.70 ± 0.58
5	9.3	1037	α-terpineol	0.12 ± 0.15
6	9.908	1074	β-linalool	1.54 ± 0.26
7	9.933	1080	citronellol	16.34 ± 1.02
8	10.163	1090	nerol	23.40 ± 2.13
9	10.242	1098	geraniol	29.20 ± 1.27
10	11.136	1157	2-methyl-6-methylene-octa-1,7-dien-3-ol	0.56 ± 0.08
11	15.061	1485	trans-farnesol	2.86 ± 0.03
	Total alcohols			83.32
			Aliphatic Hydrocarbons	
12	14.844	1448	dodecane	1.47 ± 0.02
13	17.192	1614	1-hexadecene	2.11 ± 0.24
14	17.711	1643	hexadecane	9.25 ± 0.45
	Total aliphatic hydrocarbon			12.83
			Ester	
15	11.478	1181	2,6-octadien-1-ol, 3,7-dimethyl-, acetate	0.90 ± 0.07
16	14.767	1442	n-lauryl acrylate	1.12 ± 0.15
	Total ester			2.03
			Monoterpene Hydrocarbon	
17	6.067	852.2	β-myrcene	0.05 ± 0.01
18	7.921	951	β-thujene	0.03 ± 0.02
	Total monoterpene hydrocarbon			0.08
	oxide/ether			
19	8.011	961	*trans*-rose oxide	0.08 ± 0.05
20	11.367	1167	eugenol	0.99 ± 0.01
21	11.758	1201	methyl eugenol	0.34 ± 0.11
	Total oxide/ether			1.40
			Sesquiterpene Hydrocarbon	
22	11.964	1218	β-caryophyllene	0.04 ± 0.02
23	12.125	1230	(Z,E)-α-farnesene	0.07 ± 0.00
24	12.869	1287	unknown	0.15 ± 0.00
	Total sesquiterpene hydrocarbon			0.26

of ROSE-NANO (50 and 100 mg/g emulgel, respectively), daily 1 h before the UVB exposure (Figure S1).[19]

2.5.3. UVB Exposure Test. Using UV radiation of wavelength 302 nm (CL-1000 M; UVP, Upland/CA), skin photoaging was induced. Rats were positioned on a platform and exposed to UVB radiation (the lamp was set 5 cm above the platform) at a dose of 40−80 mJ/cm^2 for exposure times of 15−30 s.[20,21] The rat's dorsal side was shaved 24 h before the experiment. Daily, the dorsal skin of the animals was visually reported and graded from 0 to 3 for the scoring of erythema[22] and wrinkles[23] (Table S2).

2.5.4. Tissue Preparation. To allow time for any acute UV effects to recuperate, biochemical assays were carried out three days following the final UV exposure.[24] At the end of the experiment, the rats were anesthetized by ketamine (85 mg/kg, i.p.) and euthanized by cervical dislocation, and the treated skin of each rat was dissected into two halves. The first half of the dorsal skin of the rats was preserved in 10% formalin for histopathological examination. The other half of the skin samples were homogenized and subjected to biochemical estimation of the antioxidant (CAT, SOD), anti-inflammatory (TNF-α, IL-6), and antiwrinkling (MMP-9) markers.

2.5.5. Biochemical Analysis. The levels of catalase (CAT) and superoxide dismutase (SOD) reactive substances were estimated in the homogenate, as reported previously.[20] The levels of interleukin 6 (IL- 6), TNF-α, and matrix metalloproteinase (MMP-9) were determined using an enzyme-linked immunosorbent assay.

2.5.6. Histopathological Studies. The skin samples from the dorsal skin of the rats were used. The samples were embedded in paraffin and formalin-fixed for histopathological analysis. They were prepared as follows: 10% neutral buffer formalin fixation, trimming, water washing, ethyl alcohol dehydration, xylene clearing, and paraffin embedding. Hematoxylin and eosin and Masson's trichrome stain (Merck Life Science) were used to prepare and stain thin slices (4−6 μm) to identify fibrous connective tissue.[25] Fixation and staining procedures were carried out as formerly stated.[26] The examination was performed using a light electric microscope (Optika B 150, Optika Microscopes, Italy)

2.5.7. Immunohistochemistry Staining Protocol. The avidin−biotin−peroxidase complex (ABC) technique was used to mount paraffin slices on positively charged slides where the Anti-Rat collagen I antibody, polyclonal antibody (Thermo Fisher Scientific, Cat# PA1-26204, Dil.: 1:200), and

https://doi.org/10.1021/acsomega.3c04756
ACS Omega 2023, 8, 33943−33954

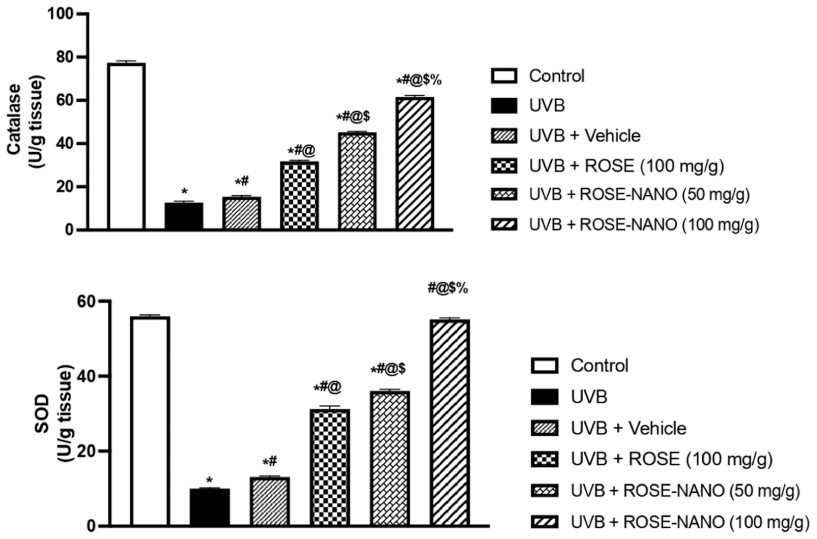

Figure 1. Effect of ROSE and ROSE-NANOs on antioxidant enzyme (SOD and CAT) levels. Values were expressed as mean ± SD. *$P < 0.05$ compared to the control group, #$P < 0.05$ compared to the ultraviolet-irradiated group, @$P < 0.05$ compared to the vehicle group, \$$P < 0.05$ compared to the ROSE emulgel group, and %$P < 0.05$ compared to ROSE-NANO (50 mg/kg) after using ANOVA, followed by Tukey's post hoc test.

Rat NFKB-P65 antibody, polyclonal antibody (Elabscience, Cat# E-AB-32232, Dil.:1:100) were assessed. The chemicals needed for the ABC technique (Vectastain ABC-HRP kit, Vector laboratories) were introduced after sections from each group were treated with these antibodies. To identify antigen−antibody complexes, markers were expressed and colored with diaminobenzidine (DAB, made by Merck Life Science). The primary or secondary antibodies were substituted with non-immune serum for the negative controls. An Olympus microscope (BX-53) was used to view IHC-stained slices.

2.5.7.1. Immunohistochemical Quantitative Analysis. Immunohistochemical expression levels of collagen A1 and NF-Kβ were assessed in six randomly chosen, non-overlapping fields using a Leica application module-operated full-HD microscopic imaging equipment (Leica Microsystems GmbH/Wetzlar/Germany)

2.5.8. Quantitative RT-PCR (Real-Time Polymerase Chain Reaction). Total RNA separated from rat dissected skin was analyzed for JNK, ERK1/2, and p38 MAPK gene expression. The RT-PCR kit (Stratagene, Cat. # 600188, La Jolla/CA) was used to prepare the complementary DNA according to the manufacturer's procedures. Using JNK, ERK1/2, and p38 MAPK primers (Table S1), quantitative RT-PCR was assessed by mixing 5 μL of complementary DNA, 12.5 μL of the SYBR Green JumpStart Taq ReadyMix (Sigma-Aldrich, Cat. # S5193, St. Louis/MO), 5.5 μL of RNAse free water, and 2 μL of each primer (5 pmol/μL).

2.5.9. Statistical Analysis. The results were represented as the average mean ± SD and were analyzed using one-way ANOVA, following Tukey's post hoc analysis. Statistical variations were considered significant at $P < 0.05$.

3. RESULTS AND DISCUSSION

3.1. Volatile oil analysis. GC/MS analysis of volatile constituents of *R. damascena* (Table 1) led to the identification of 24 constituents classified into six different classes including alcohols (83.3%), aliphatic hydrocarbons (12.8%), esters (2.03%), monoterpene hydrocarbon (0.08%), oxide/ether (1.4%), and sesquiterpene hydrocarbon (0.26; Figures S2 and S3). Alcohols were the most prominent class of volatile constituents in Taif rose oil, where geraniol, nerol, citronellol, phenyl ethyl alcohol, and linalool represented 29.2, 23.4, 16.34, 4.96, and 3.24%, respectively. Meanwhile, hexadecane was the predominant aliphatic hydrocarbon (9.25%). The obtained results agree with previously published data on Taif rose oil, which showed prominence of β-citronellol, nerol, geraniol, and linalool in addition to phenyl ethyl alcohol, which plays a remarkable role in rose odor.[4,27]

3.2. In Vitro Characterization of ROSE-NANO. The *z*-average diameter of the developed ROSE-NANO was 125.5 ± 3.7 nm. The relatively low observed PDI value of 0.167 ± 0.008 nm indicates good homogeneity and high kinetic stability of the developed formulation.[28]

3.3. UVB Exposure Test. The effect of topical ROSE emulgel, ROSE-NANO, and plain NANO formulations on UV-induced photoaging was assessed visually on dorsal mouse skin. The results (Figure S4) showed that the non-UV-irradiated group had undamaged skin with a smooth surface (group 1). Meanwhile, the occurrence of irritation and inflammation in the UV-irradiated group (group 2) was proved through increasing skin thickness and the appearance of scars. Plain NANO formulation (group 3) with slightly enhanced skin inflammation was observed in group 2, which may be attributed to the photoprotective effect of α-CD.[29,30] Application of ROSE formulation (group 4) showed slight enhancement of rat skin. Meanwhile, the prepared ROSE-NANO at both tested concentrations (50 and 100 mg/g emulgel) revealed protective and prophylactic effects on the skin, where higher oil concentrations showed higher potency. This could be explained by NANOs' penetration enhancer function, which improves the permeability of the drug through the stratum corneum barrier. Moreover, the reported interaction of cyclodextrin with skin keratocytes may result in higher retention of the prepared formula in the skin in comparison to the free rose oil.[31,32] As a result, our findings highlight the NANO formulation's potential to keep medication deeply in the skin layers, which is consistent with the current study's essential goal; therefore, ROSE-NANOs can be proposed as a viable topical antiaging tool.

In this study, the hairless dorsal skin of rats was used as an experimental model for the photoaging study. During the

https://doi.org/10.1021/acsomega.3c04756
ACS Omega 2023, 8, 33943−33954

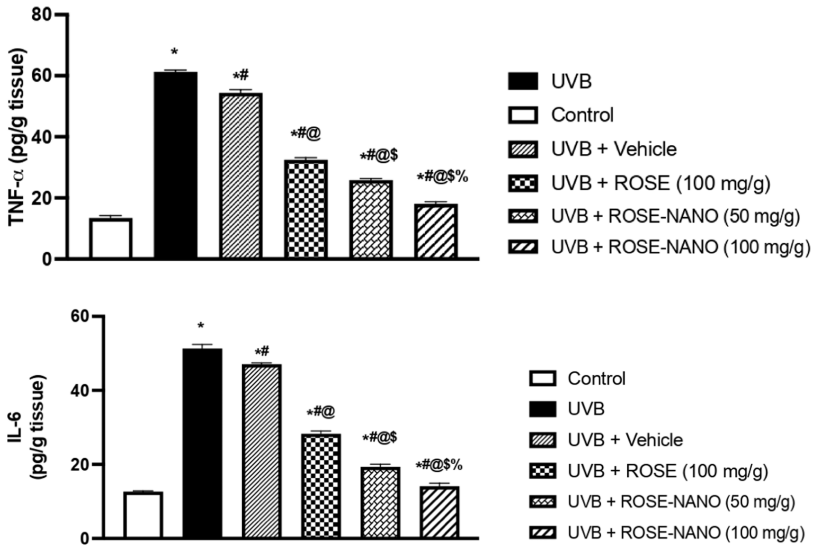

Figure 2. Effect of ROSE and ROSE-NANOs on the proinflammatory cytokines (IL-6 and TNF-α). Values were expressed as mean ± SD. *$P < 0.05$ compared to the control group, #$P < 0.05$ compared to the ultraviolet-irradiated group, @$P < 0.05$ compared to the vehicle group, \$$P < 0.05$ compared to the ROSE emulgel group, and %$P < 0.05$ compared to ROSE-NANO (50 mg/kg) after using ANOVA, followed by Tukey's post hoc test.

experiment, the dorsal skin of animals was visually examined daily and scored for erythema[22,33] and wrinkles[23,34] according to the scoring scale (Table S2).

As illustrated in the Supporting Information (Table S3), at day 1, no phototoxic signs can be noticed in all groups. At day 1, no phototoxic signs were noticed in all groups except in the positive control group, which showed clear signs starting from the first day of exposure. At day 3, signs of phototoxicity began to appear in all of the groups exposed to UVB radiation. In all groups, the toxic reactions of UVB irradiation were increased by increasing the period of exposure. It is clear that all treated groups (groups 3, 4, 5, and 6) showed a lower incidence of phototoxic effects than the positive control group (p 0.05). Groups 3 and 4 showed the lowest skin protection effects, concerning both the antierythematic and antiwrinkle effects (p 0.05), proving that using higher essential oil concentrations had a beneficial effect on the suppression of the phototoxic effects.

Dorsal parts of the rats' skin under study were visually examined at the end of the experiment.

Intact skin with a smooth surface was observed in the negative control group. On the other hand, thick and deep wrinkles with projecting scars were obvious after UVB irradiation. This was improved by the pre-application of suspensions, where only few wrinkle and scar traces were observed. Interestingly, pre-application of the formula offered high prophylactic and protective effects, and skin appeared intact and clear from any inflammatory or wrinkling sign.

3.4. Biochemical Analysis. Skin damage is a result of unprotected exposure to UVB radiation, and other biochemical indicators can be used to further prove this. The indicated protective impact of the produced ROSE-NANOs was assessed in the current investigation by assessing the levels of biochemical markers for antioxidant, anti-inflammatory, and antiwrinkle activities.

3.4.1. Effect of ROSE-NANO on the Antioxidant Markers on UVB-Irradiated Rats. Reactive oxygen species (ROS) is responsible for UVB-induced cell death due to its ability to transfer electromagnetic energy from UVB light to molecular oxygen, causing skin damage.[10,24] This study showed the ability of ROSE emulgel and ROSE-NANOs to reduce the level of antioxidant enzymes, as displayed in Figure 1. The findings of the present study revealed that exposure to ultraviolet rays resulted in a significant reduction of antioxidant enzymes in the UVB-irradiated group (group 2) by 2.3-fold, which is in line with earlier studies.[20] Topical application of the ROSE formula (group 4) caused a significant reduction of the antioxidant levels (CAT and SOD) in comparison to the UVB-irradiated group (group 2) by 1.5- and 1.4-fold, respectively, confirming the antioxidant activity of the oil. UVB exposure induces direct inflammation and proliferation in human and animal skin and produces reactive oxygen species indirectly by depleting the antioxidants in the skin.[35] Moreover, exposure of mammalian cells to UVB causes the generation of reactive oxygen species, which is considered one of the major alterations that lead to deleterious outcomes.[36] Topical application of the prepared formula (groups 5 and 6) significantly improved the oxidative stress by decreasing CAT and SOD by 1.6- and 1.3-fold, respectively, in comparison to ROSE oil.

This effect was also confirmed during visual inspection of the skin rat after treatment. The antioxidant activity of ROSE is well established through its active compounds. The oil inhibited hexanal oxidation by 100% at 100 μg/mL, scavenged the DPPH radical by 70%, and inhibited malondialdehyde formation from squalene upon UV irradiation by 46%.[37] The observed antioxidant effect of the oil could be attributed to its major constituents of geraniol (29.2%), nerol (23.4%), citronellol (16.34%), phenyl ethyl alcohol (4.96%), and linalool (3.24%). It was reported that citronellol, nerol, and geraniol inhibited malondialdehyde formation at 1000 ppm concertation by 27.5, 42.7, and 34.9, respectively, in the thiobarbituric acid assay.[37] Meanwhile, linalool was reported to have a strong radical scavenging activity in the DPPH assay.[38] The obtained results confirmed the advantage of the prepared NANO formula over regular emulgel as skin antiaging through antioxidant activity.

3.4.2. Effect of ROSA-NANO on Anti-Inflammatory Markers on UVB-Irradiated Rats. Exposing rat skin to ultraviolet irradiation resulted in the release of proinflammatory cytokine (IL-6 and TNF-α), causing skin damage as displayed in the UV-irradiated group (group 2) that showed a significant increase in proinflammatory cytokine (IL-6 and TNF-α) by 2.4- and 2.3-

https://doi.org/10.1021/acsomega.3c04756
ACS Omega 2023, 8, 33943−33954

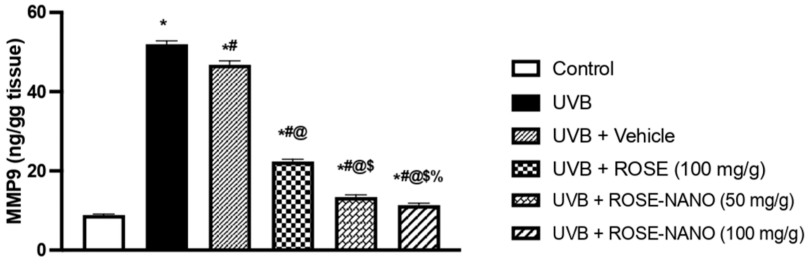

Figure 3. Effect of ROSE and ROSE-NANOs on the production of MMPs. Values were expressed as mean ± SD. $^{*}P < 0.05$ compared to the control group, $^{\#}P < 0.05$ compared to the ultraviolet-irradiated group, $@P < 0.05$ compared to the vehicle group, $^{\$}P < 0.05$ compared to the ROSE emulgel group, and $^{\%}P < 0.05$ compared to ROSE-NANO (50 mg/kg) after using ANOVA, followed by Tukey's post hoc test.

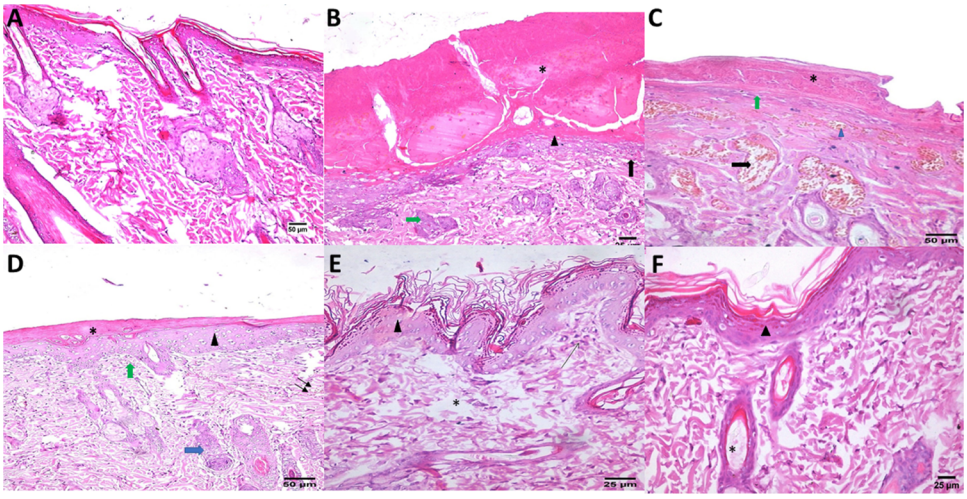

Figure 4. Microscopic examination of histological features in different skin tissues (hematoxylin and eosin stain). (A) Normal histological structure of the skin. (B) Replacement of the prickle cell layer (star) by fibrous connective tissue, partial formation of some epidermal layers (arrowhead), formation of migratory epidermal cells (green arrow) with focal infiltration by mononuclear inflammatory cells (black arrow), and congestion of dermal blood vessels (black arrow). (C) Partial loss of the prickle cell layer (star) with formation of some epidermal layers (green arrow), the presence of dermal blood vessel congestion (black arrow), and the presence of dermal hemorrhage (arrowhead). (D) Partial loss of the prickle cell layer (star) with formation of some epidermal layers (arrowhead) and migratory epidermal cells (blue arrow) and the presence of mononuclear inflammatory cells (green arrow) with hemorrhage (double arrow) in the dermis. (E) Formation of some epidermal layers (arrowhead) with dermal edema (star) and the presence of the focal area of mononuclear inflammatory cells (arrow). (F) Formation of the epidermal layer (arrowhead) and migratory epidermal cells (star). A: Control, non-UVB-irradiated group; B: UVB-irradiated group; C: vehicle group; D: ROSE emulgel group; E: ROSE-NANO (50 mg/kg); and F: ROSE-NANO (100 mg/kg).

fold, respectively, in comparison to a nonirradiated group (group 1; Figure 2). Topical application of either ROSE formula or ROSE-NANO exerts significant anti-inflammatory activity. In comparison to the UV-irradiated group (group 2), ROSE emulgel (group 4) caused a significant decrease in the levels of IL-6 and TNF-α by 1.3- and 1.4-fold, respectively. This result is in agreement with previously published data that reported folk use of ROSE as an anti-inflammatory[39] and its ability to suppress COX-2 in vitro.[40] In addition, it was observed that the plain NANO formulation (group 3) also exerts anti-inflammatory activity by decreasing IL-6 and TNF-α by 1.2- and 1.7-fold, respectively, which may be attributed to the protective and defending effects of the nanosystem.[41] Finally, ROSE-NANO groups (5 and 6) displayed promising anti-inflammatory activity that was evident through a significant decrease in IL-6 and TNF-α. As discussed before, the obtained results confirmed the advantage of the prepared NANO formula in enhancing drug solubility, warranting improvement of skin penetration and the photoprotective effect.

Moreover, the major constituents in ROSE were also reported for their significant anti-inflammatory activity. Citronellol is reported to inhibit the production of NO and PGE2 in RAW 264.7 macrophage through inhibition of iNOS enzyme activity. In addition, it also suppresses the production of COX-2 in LPS-induced inflammation and activated PPAR α and γ.[40] Moreover, nerol showed a significant decrease in the level of inflammatory cytokines (IL-13 and TNF-α) in oxazolone-induced colitis.[42] Linalool can also reduce edema and exert strong anti-inflammatory activity in the carrageenan-induced rat edema model, which could be attributed to its ability to reduce levels of leukotrienes.[40] Phenethyl alcohol also proved anti-inflammatory activity in topical application by decreasing TNF-α and NF-κB protein expressions in addition to its antioxidant activity.[43] Based on these results, ROSE-NANO plays a unique function in preventing photoaging in the skin by lowering IL-6 and TNF-α levels, which work in tandem with ROSE's photoprotective effect.

3.4.3. Antiwrinkling Markers. Exposure to ultraviolet radiation stimulates the generation of free radicals, which raises the synthesis of MMPs, resulting in the degeneration of elastin and collagen networks and finally leading to skin wrinkling.[44,45] Ultraviolet radiation produced wrinkle formation due to the degradation of the three-dimensional fiber network under the effect of IL-1 and the granulocyte-macrophage colony-

https://doi.org/10.1021/acsomega.3c04756
ACS Omega 2023, 8, 33943−33954

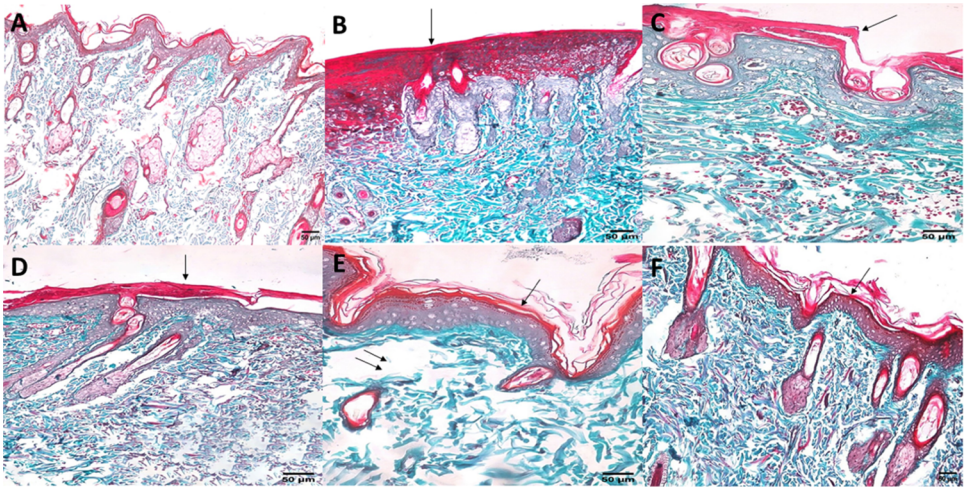

Figure 5. Microscopic examination of histological features in different skin samples using the Masson trichrome stain. (A) Normal histological structure of the skin. (B) Loss of the prickle cell layer with partial formation of some epidermal layers (black arrow). (C) Partial loss of the prickle cell layer with formation of some epidermal layers and migratory epidermal cells (black arrow). (D) Partial loss of the prickle cell layer with formation of some epidermal layers and migratory epidermal cells (black arrow). (E) Formation of some epidermal layers and migratory epidermal cells (black arrow) with dermal edema (double arrow). (F) Formation of all layers of the epidermis and migratory epidermal cells. A: Control, non-UVB-irradiated group; B: UVB-irradiated group, C: vehicle group; D: ROSE emulgel group; E: ROSE-NANO (50 mg/kg); and F: ROSE-NANO (100 mg/kg).

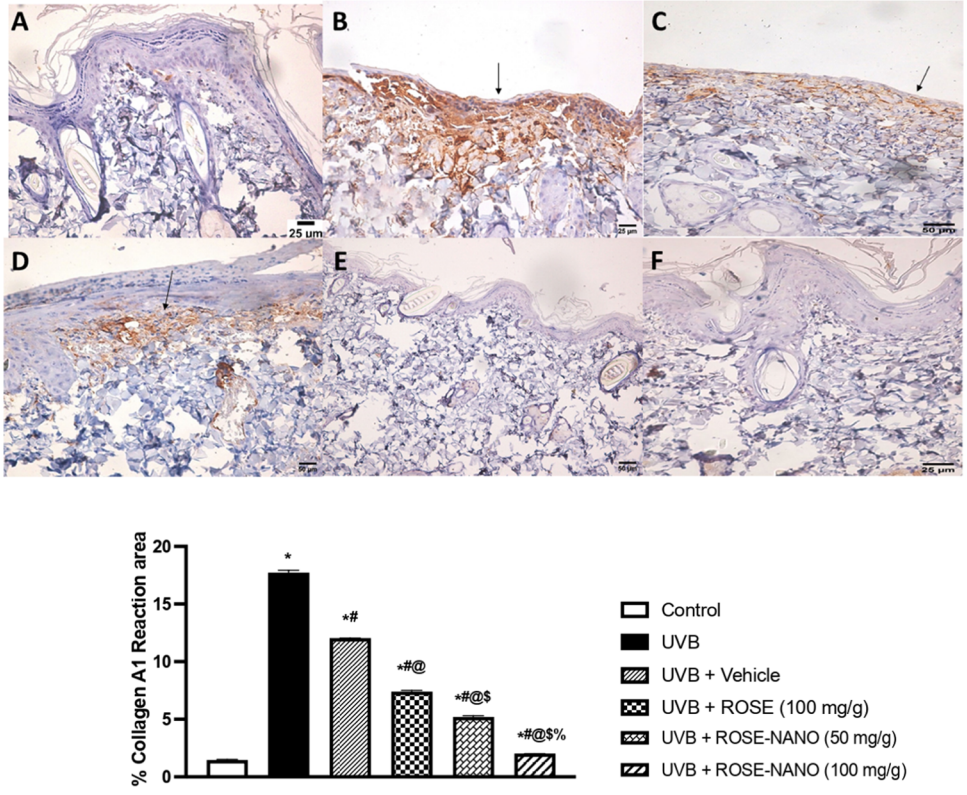

Figure 6. Immunohistochemical expression of collagen I in the skin of irradiated and treated groups, showing a negative reaction in (A), a strongly positive reaction in (B), a moderate reaction in (C, D), and a negative reaction in (E, F) (IHC-peroxidase—DAB). A: Control, non-UVB-irradiated group; B: UVB-irradiated group; C: vehicle group; D: ROSE emulgel group; E: ROSE-NANO (50 mg/kg); and F: ROSE-NANO (100 mg/kg) $^{*}P < 0.05$ compared to the control group, $^{\#}P < 0.05$ compared to the ultraviolet-irradiated group, $@P < 0.05$ compared to the vehicle group, $^{\$}P < 0.05$ compared to the ROSE emulgel group, and $^{\%}P < 0.05$ compared to ROSE-NANO (50 mg/kg) after using ANOVA, followed by Tukey's post hoc test.

stimulating factor.[46,47] The obtained results, Figure 3, revealed the elevation of MMP-9 (antiwrinkling marker) in the irradiated group by 3.2-fold from the control group. Meanwhile, ROSE emulgel as well as ROSE-NANO groups exerted significant reduction in MMP-9 with the superior activity of the prepared NANO formula by 1.6-fold over the oil formula. The antiwrinkle effect of the oil could be attributed mainly to its radical scavenging activity as well as its anti-inflammatory effect, as discussed before. In consequence, collagen fragmentation was prevented due to a reduction in MMP-9 production in fibroblasts.[10,24] Furthermore, collagen and hyaluronic acid as major components of the dermis and epidermis (which are non-

https://doi.org/10.1021/acsomega.3c04756
ACS Omega 2023, 8, 33943−33954

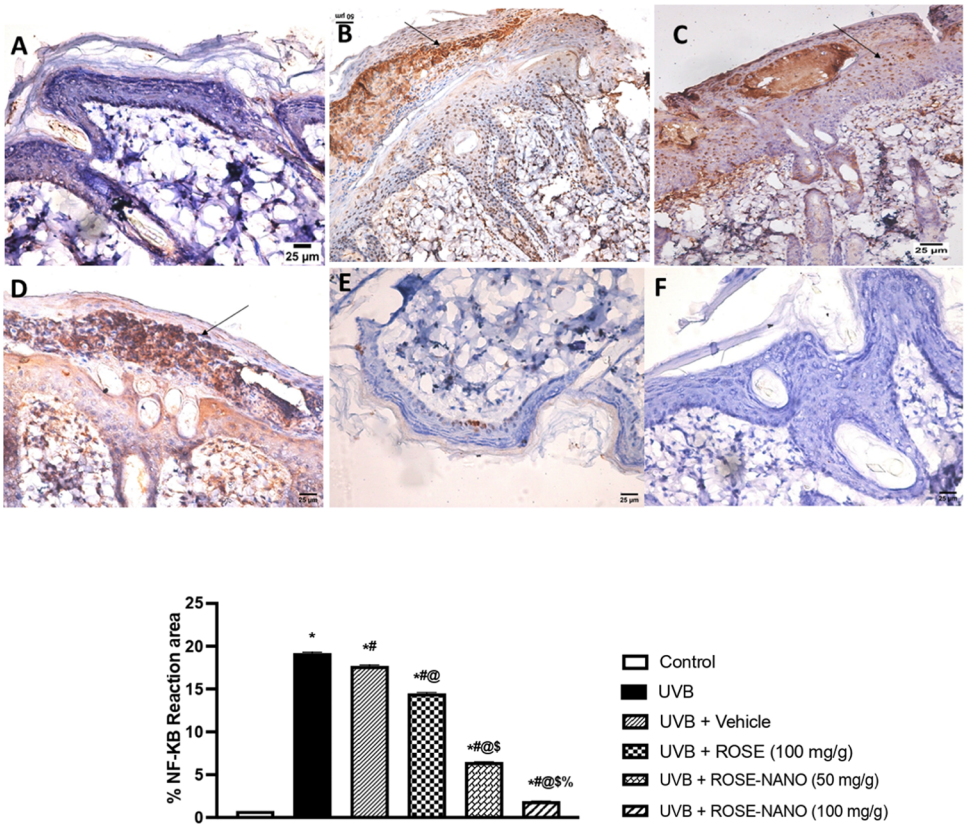

Figure 7. Immunohistochemical expression of NF-κB in the skin of irradiated and treated groups showing s negative reaction in (A), a strongly positive reaction in nuclei of epidermis in (B−D) (black arrows), a mild reaction in (E) (black arrow), and a negative reaction in (F) (IHC-peroxidase—DAB). A: Control, non-UVB-irradiated group; B: UVB-irradiated group: C: vehicle group; D: ROSE emulgel group; E: ROSE-NANO (50 mg/kg); and F: ROSE-NANO (100 mg/kg). Values were expressed as mean ± SD. $^{*}P < 0.05$ compared to the control group, $^{\#}P < 0.05$ compared to the ultraviolet-irradiated group, $@P < 0.05$ compared to the vehicle group, $^{\$}P < 0.05$ compared to the ROSE emulgel group, and $^{\%}P < 0.05$ compared to ROSE-NANO (50 mg/kg) after using ANOVA, followed by Tukey's post hoc test.

fibrous) also contribute to dryness protection. Moreover, a decrease in hyaluronic acid production and collagen cleavage has also been reported following UVB skin irradiation. Therefore, it could be concluded that ROSE could prevent hyaluronic acid degradation by inhibiting hyaluronidase activation.[48]

In conclusion, biochemical studies have indicated that ROSE-NANO formulations have superior antiaging properties to free drugs and plain NANO formulations.

3.5. Histopathological Examination. Microscopic histopathological examination by using the H&E stain of skin samples isolated from the control group showed typical histological properties of epidermal layers. It revealed intact keratinocytes, an intact dermal layer, limited inflammatory cell infiltrates, and normal vasculature (Figure 4A). On the other side, the ultraviolet-irradiated group demonstrated an increase in the thickness of the epidermal layer, shrinking of keratinocytes nucleus, cytoplasmic vacuolation, and formation of apoptotic bodies (Figure 4B). The ROSE emulgel, as well as ROSE-NANO-treated groups in both concentrations, revealed almost consistent morphological characteristics with partial protective efficacy.

Intact epidermal layers with evident normal keratinocytes were shown in these groups with a marked decline in the epidermal thickness. Further, dermal layers displayed minimal inflammatory cell infiltrates with minimal records of congested blood (Figure 4D−F). Microscopic histopathological examination of skin samples using the Masson trichome stain showed severe loss of the prickle cell layer and its replacement by fibrous connective tissue as well as inflammatory cell infiltrates in the UVB-irradiated group compared to the normal nonirradiated control group (Figure 5A,B).

3.6. Immunohistochemical Quantitative Analysis of Collagen I and NF-κB. Significant reduction in collagen I fibers was observed in both ROSE-NANO-treated groups at both concentrations (Figure 6E,F) relative to the control irradiated group, while no significant effect was observed in the ROSE-treated group (Figure 6D). Moreover, in comparison to the ultraviolet-irradiated group, ROSE emulgel and ROSE-NANO groups showed a significant decrease in positively stained subepidermal elastic fibers. (Figure 6E,F).

Quantitative analysis of NF-Kβ immunoreactivity is done in different groups as a tool to identify the proliferation of the inflammatory insult in different layers of the skin of rats after UVB irradiation and treatment with different preparations. Immunohistochemical examination demonstrated that the average number of skin NF-Kβ cells was greatly higher by 8-fold in the model UVB-irradiated rats as compared with the nonirradiated group. This dramatic elevation in the proinflammatory cytokines proved a marked insult to different skin layers following the UVB irradiation. Conversely, the mean number of skin NF-Kβ cells decreased significantly by 3.4, 7.2, 14.2, and 17% in groups 3, 4, 5, and 6 treated groups, respectively, compared with the mean model-induced group. These results revealed a significant improvement in the

https://doi.org/10.1021/acsomega.3c04756
ACS Omega 2023, 8, 33943−33954

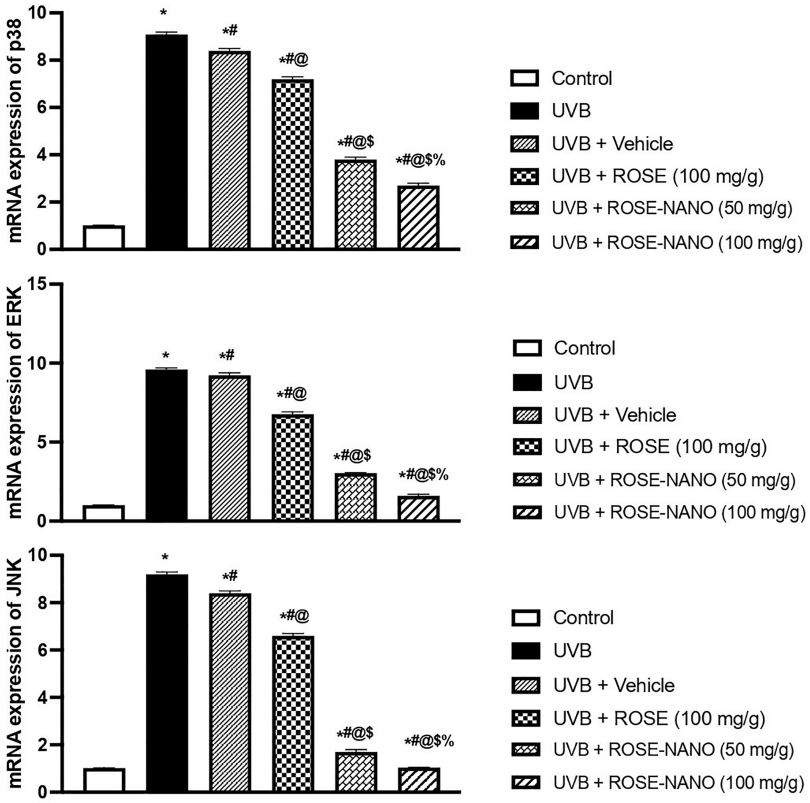

Figure 8. ERK1/2, JNK, and p38 MAPK levels assessed by PCR in the rat skin. Values are expressed as mean ± SD; $n = 3$. Statistical analyses were performed using one-way analysis of variance (ANOVA), followed by Tukey's post hoc test. Values were expressed as mean ± SD. $^{*}P < 0.05$ compared to the control group, $^{\#}P < 0.05$ compared to the ultraviolet-irradiated group, $@P < 0.05$ compared to the vehicle group, $^{\$}P < 0.05$ compared to the ROSE emulgel group, and $^{\%}P < 0.05$ compared to ROSE-NANO (50 mg/kg) after using ANOVA, followed by Tukey's post hoc test.

inflammatory pattern of the skin of animals exposed to UVB irradiation when treated with ROSE-NANO preparations (Figure 7).

3.7. Quantitative RT-PCR Analysis of JNK, ERK, and p38 MAPK Signaling. MAPKs (mitogen-activated protein kinases) are a group of protein kinases accountable for cytokine gene expression, apoptosis, cell proliferation, and metalloproteinase production.[49] Furthermore, the MAPK pathway regulates the synthesis of proinflammatory cytokines.[50] In this work, three main MAP kinase families, ERK, JNK, and p38, were evaluated (Figure 8), where p38 is included in the production of cytokine[51] while inflamed and damaged skin are caused by JNK and ERK signaling.[52]

The obtained results revealed high expression of JNK, ERK1/2, and p38 MAPK genes in the irradiated group, while ROSE emulgel and ROSE-NANO groups showed lower expression of these genes. Furthermore, no notable variations were observed between the ROSE-NANO groups and the negative control group.

4. CONCLUSIONS

Exposure of the skin to ultraviolet rays accelerates the appearance of aging signs. Exposure to UV radiation resulted in severe oxidative stress due to the production of ROS. These signs appear because ultraviolet radiation causes a deficiency of antioxidants and a reduction in anti-inflammatory and anti-wrinkling markers. Therefore, topical application of antioxidants protects skin from photoaging. In this regard, the use of natural skin care products is one of the safest alternatives to synthetic ones due to their lack of side effects. Moreover, a nano-formulation of natural products will increase the solubility of the active compound, improve skin penetration, and provide photoprotection. In this work, ROSE emulgel (100 mg/g), as well as the prepared ROSE-NANO formulations, was applied topically on the rat skin at two dose levels (50 and 100 mg/g emulgel) to study their possible protective effect against UVB-induced photoaging in adult male Wistar rats. The prepared nanocomposite was able to reduce the signs of aging in the group irradiated with ultraviolet radiation more effectively than ROSE emulgel through improvement in the antioxidant markers levels, namely, CAT and SOD, decreasing the level of the inflammatory markers. The protective effect could be referred to the reported antioxidant and anti-inflammatory effects of major constituents in rose oil ROSE, including geraniol (29.2%), nerol (23.4%), citronellol (16.34%), phenyl ethyl alcohol (4.96%), and linalool (3.24%). Moreover, the prepared formula prevents collagen fragmentation through the reduction of MMP-9 in fibroblasts where ROSE-NANO formulations were superior to ROSE emulgel. In addition, the expression of NF-KB, ERK1/2, JNK, and p38 MAPK genes decreased significantly. Finally, the current study demonstrates that ROSE-NANOs were successfully designed to overcome ROSE delivery barriers within the skin and to prove their efficacy against UV-induced oxidative damage and skin aging as skin photoprotectants. Furthermore, the nanoformulation of rose oil may be able to deliver the same amount of the oil as the traditional application but with a much smaller dose. This can lead to cost savings for both patients and healthcare providers.

https://doi.org/10.1021/acsomega.3c04756
ACS Omega 2023, 8, 33943−33954

■ ASSOCIATED CONTENT

Supporting Information

The Supporting Information is available free of charge at https://pubs.acs.org/doi/10.1021/acsomega.3c04756.

Diagram showing the experimental design (Figure S1); GC/MS chromatogram of the essential oil of *R. damascena* Miller (Taif rose) (Figure S2); relative concertation of different volatile constituents in *R. damascena* Miller (Taif rose) (Figure S3); photographs of the dorsal skin of the rats. Group 1: control, group 2: UVB-irradiated group, group 3: vehicle group, group 4: ROSE emulgel group, and groups 5 and 6: ROSE-NANO (50 and 100 mg/kg, respectively) (Figure S4); primer sequences for the genes used for polymerase chain reaction investigation (Table S1); scoring system for the evaluation of skin reactions, after UVB exposure (Table S2); and effect of UVB exposure on the hairless skin of adult male Wistar rats (Table S3) (PDF)

■ AUTHOR INFORMATION

Corresponding Author

Hossam M. Abdallah − *Department of Natural Products and Alternative Medicine, Faculty of Pharmacy, King Abdulaziz University, Jeddah 21589, Saudi Arabia;* orcid.org/0000-0002-0234-7492; Email: hmafifi@kau.edu.sa

Authors

Abdulrahman E. Koshak − *Department of Natural Products and Alternative Medicine, Faculty of Pharmacy, King Abdulaziz University, Jeddah 21589, Saudi Arabia*

Mohamed A. Farag − *Department of Pharmacognosy, Faculty of Pharmacy, Cairo University, Giza 11562, Egypt;* orcid.org/0000-0001-5139-1863

Nesrine S. El Sayed − *Department of Pharmacology and Toxicology, Faculty of Pharmacy, Cairo University, Cairo 11562, Egypt*

Shaimaa M. Badr-Eldin − *Department of Pharmaceutics, Faculty of Pharmacy, King Abdulaziz University, Jeddah 21589, Saudi Arabia*

Osama A. A. Ahmed − *Department of Pharmaceutics, Faculty of Pharmacy, King Abdulaziz University, Jeddah 21589, Saudi Arabia*

Mardi M. Algandaby − *Department of Biological Sciences, Faculty of Science, King Abdulaziz University, Jeddah 21589, Saudi Arabia*

Ashraf B. Abdel-Naim − *Department of Pharmacology and Toxicology, Faculty of Pharmacy, King Abdulaziz University, Jeddah 21589, Saudi Arabia*

Sabrin R. M. Ibrahim − *Department of Chemistry, Preparatory Year Program, Batterjee Medical College, Jeddah 21442, Saudi Arabia; Department of Pharmacognosy, Faculty of Pharmacy, Assiut University, Assiut 71526, Egypt;* orcid.org/0000-0002-6858-7560

Gamal A. Mohamed − *Department of Natural Products and Alternative Medicine, Faculty of Pharmacy, King Abdulaziz University, Jeddah 21589, Saudi Arabia*

Peter Proksch − *Institute of Pharmaceutical Biology and Biotechnology, Heinrich-Heine-Universität Düsseldorf, 40225 Düsseldorf, Germany*

Haidy Abbas − *Department of Pharmaceutics, Faculty of Pharmacy, Damanhour University, Damanhour 43211, Egypt*

Complete contact information is available at: https://pubs.acs.org/10.1021/acsomega.3c04756

Funding

This project was funded by the Deanship of Scientific Research (DSR) at King Abdulaziz University, Jeddah, Saudi Arabia, under grant no. (RG-3-130-42). The authors, therefore, acknowledge with thanks DSR's technical and financial support.

Notes

The authors declare no competing financial interest.

■ REFERENCES

(1) Zhao, C.-Y.; Xue, J.; Cai, X.-D.; Guo, J.; Li, B.; Wu, S. Assessment of the key aroma compounds in rose-based products. *J. Food Drug Anal.* **2016**, *24*, 471−476.

(2) Sarkic, A.; Stappen, I. Essential oils and their single compounds in cosmetics—A critical review. *Cosmetics* **2018**, *5*, 11.

(3) Akram, M.; Riaz, M.; Munir, N.; Akhter, N.; Zafar, S.; Jabeen, F.; Ali Shariati, M.; Akhtar, N.; Riaz, Z.; Altaf, S. H.; et al. Chemical constituents, experimental and clinical pharmacology of *Rosa damascena*: a literature review. *J. Pharm. Pharmacol.* **2020**, *72*, 161−174.

(4) Kurkcuoglu, M.; Baser, K.; Akterian, S.; Fidan, H.; Stoyanova, A. Chemical composition, sensory evaluation and antimicrobial activity of Taif rose (*Rosa damascena* Mill.) essential oils. *Bulg. Chem. Commun.* **2020**, *52*, 460−466.

(5) Mohsen, E.; Younis, I. Y.; Farag, M. A. Metabolites profiling of Egyptian *Rosa damascena* Mill. flowers as analyzed via ultra-high-performance liquid chromatography-mass spectrometry and solid-phase microextraction gas chromatography-mass spectrometry in relation to its anti-collagenase skin effect. *Ind. Crops Prod.* **2020**, *155*, No. 112818.

(6) Mahboubi, M. *Rosa damascena* as holy ancient herb with novel applications. *J. Tradit. Complement. Med.* **2016**, *6*, 10−16.

(7) Motule, A. S.; More, M. P.; Manwar, J. V.; Wadekar, A. B.; Gudalwar, B. R. Ethnopharmacological relevance's of herbal plants used in cosmetics and toiletries preparations. *GSC Biol. Pharm. Sci.* **2021**, *16*, 241−263.

(8) Park, B.; Hwang, E.; Seo, S. A.; Zhang, M.; Park, S.-Y.; Yi, T.-H. Dietary *Rosa damascena* protects against UVB-induced skin aging by improving collagen synthesis via MMPs reduction through alterations of c-Jun and c-Fos and TGF-β1 stimulation mediated smad2/3 and smad7. *J. Funct. Foods* **2017**, *36*, 480−489.

(9) Stojiljković, D.; Pavlović, D.; Arsić, I. Oxidative stress, skin aging and antioxidant therapy. *Acta Fac. Med. Naissensis* **2014**, *31*, 207−217.

(10) Gendrisch, F.; Esser, P. R.; Schempp, C. M.; Wölfle, U. Luteolin as a modulator of skin aging and inflammation. *BioFactors* **2021**, *47*, 170−180.

(11) Shukla, S. K.; Chan, A.; Parvathaneni, V.; Gupta, V. Metformin-loaded chitosomes for treatment of malignant pleural mesothelioma - A rare thoracic cancer. *Int. J. Biol. Macromol.* **2020**, *160*, 128−141.

(12) Seo, J. Y.; Kim, E. K.; Lee, S. H.; Park, K. C.; Kim, K. H.; Eun, H. C.; Chung, J. H. Enhanced expression of cylooxygenase-2 by UV in aged human skin in vivo. *Mech. Ageing Dev.* **2003**, *124*, 903−910.

(13) Shanbhag, S.; Nayak, A.; Narayan, R.; Nayak, U. Y. Anti-aging and sunscreens: paradigm shift in cosmetics. *Adv. Pharm. Bull.* **2019**, *9*, 348.

(14) Elsheikh, M. A.; Gaafar, P. M. E.; Khattab, M. A.; A Helwah, M. K.; Noureldin, M. H.; Abbas, H. Dual-effects of caffeinated hyalurosomes as a nano-cosmeceutical gel counteracting UV-induced skin ageing. *Int. J. Pharm.* **2023**, *5*, No. 100170.

(15) Fuchs, J. Potentials and limitations of the natural antioxidants RRR-alpha-tocopherol, L-ascorbic acid and β-carotene in cutaneous photoprotection. *Free Radicals Biol. Med.* **1998**, *25*, 848−873.

(16) Farag, M. A.; El-Kersh, D. M. Volatiles profiling in *Ceratonia siliqua* (Carob bean) from Egypt and in response to roasting as analyzed via solid-phase microextraction coupled to chemometrics. *J. Adv. Res.* **2017**, *8*, 379−385.

(17) Inoue, M.; Hashizaki, K.; Taguchi, H.; Saito, Y. Formation and characterization of emulsions using β-cyclodextrin as an emulsifier. *Chem. Pharm. Bull.* **2008**, *56*, 668−671.
(18) Badr-Eldin, S. M.; Labib, G. S.; Aburahma, M. H. Eco-Friendly tadalafil Surfactant-Free dry emulsion tablets (SFDETs) stabilized by in situ self-assembled aggregates of natural oil and native cyclodextrins. *AAPS PharmSciTech* **2019**, *20*, No. 255.
(19) Nayebi, N.; Khalili, N.; Kamalinejad, M.; Emtiazy, M. A systematic review of the efficacy and safety of Rosa damascena Mill. with an overview on its phytopharmacological properties. *Complement. Ther. Med.* **2017**, *34*, 129−140.
(20) Abbas, H.; Kamel, R.; El-Sayed, N. Dermal anti-oxidant, anti-inflammatory and anti-aging effects of Compritol ATO-based Resveratrol colloidal carriers prepared using mixed surfactants. *Int. J. Pharm.* **2018**, *541*, 37−47.
(21) Schaffler, K.; Nicolas, L. B.; Borta, A.; Brand, T.; Reitmeir, P.; Roebling, R.; Scholpp, J. Investigation of the predictive validity of laser-EPs in normal, UVB-inflamed and capsaicin-irritated skin with four analgesic compounds in healthy volunteers. *Br. J. Clin. Pharmacol.* **2017**, *83*, 1424−1435.
(22) Mackenzie, L. A.; Frain-Bell, W. The construction and development of a grating monochromator and its application to the study of the reaction of the skin to light. *Br. J. Dermatol.* **1973**, *89*, 251−264.
(23) Bissett, D.; Hannonand, D.; Orr, T. An animal model of solar-aged skin: histological, physical, and visible changes in UV-irradiated hairless mouse skin. *Photochem. Photobiol.* **1987**, *46*, 367−378.
(24) Kim, S. R.; Jung, Y. R.; An, H. J.; Kim, D. H.; Jang, E. J.; Choi, Y. J.; Moon, K. M.; Park, M. H.; Park, C. H.; Chung, K. W. Anti-wrinkle and anti-inflammatory effects of active garlic components and the inhibition of MMPs via NF-κB signaling. *PLoS One* **2013**, *8*, No. e73877.
(25) Suvarna, K. S.; Layton, C.; Bancroft, J. D. *Bancroft's Theory and Practice of Histological Techniques E-Book*; Elsevier health sciences, 2018.
(26) Culling, C. F. A. *Handbook of Histopathological and Histochemical Techniques: Including Museum Techniques*; Butterworth-Heinemann, 2013.
(27) Abdel-Hameed, E.-S. S.; Bazaid, S. A.; Hagag, H. A. Chemical characterization of *Rosa damascena* Miller var. *trigintipetala* Dieck essential oil and its in vitro genotoxic and cytotoxic properties. *J. Essent. Oil Res.* **2016**, *28*, 121−129.
(28) Chong, W.-T.; Tan, C.-P.; Cheah, Y.-K.; B Lajis, A. F.; Habi Mat Dian, N. L.; Kanagaratnam, S.; Lai, O.-M. Optimization of process parameters in preparation of tocotrienol-rich red palm oil-based nanoemulsion stabilized by Tween80-Span 80 using response surface methodology. *PLoS One* **2018**, *13*, No. e0202771.
(29) van Hoogevest, P.; Fahr, A. Phospholipids in Cosmetic Carriers. In *Nanocosmetics: From Ideas to Products*; Cornier, J., Keck, C., Van de Voorde, M., Eds; 2019, pp 95−140. DOI: 10.1007/978-3-030-16573-4_6
(30) Loukas, Y. L.; Jayasekera, P.; Gregoriadis, G. Characterization and Photoprotection Studies of a Model. gamma.-Cyclodextrin-Included Photolabile Drug Entrapped in Liposomes Incorporating Light Absorbers. *J. Phys. Chem. A* **1995**, *99*, 11035−11040.
(31) El-Nabarawi, M. A.; Shamma, R. N.; Farouk, F.; Nasralla, S. M. Bilosomes as a novel carrier for the cutaneous delivery for dapsone as a potential treatment of acne: preparation, characterization and in vivo skin deposition assay. *J. Liposome Res.* **2020**, *30*, 1−11.
(32) Mosallam, S.; Sheta, N. M.; Elshafeey, A. H.; Abdelbary, A. A. Fabrication of highly deformable bilosomes for enhancing the topical delivery of terconazole: in vitro characterization, microbiological evaluation, and in vivo skin deposition study. *AAPS PharmSciTech* **2021**, *22*, No. 74.
(33) Fuchs, J.; Kern, H. Modulation of UV-light-induced skin inflammation by D-alpha-tocopherol and L-ascorbic acid: a clinical study using solar simulated radiation. *Free Radical Biol. Med.* **1998**, *25*, 1006−1012.
(34) Kamel, R.; Abbas, H.; Fayez, A. Diosmin/essential oil combination for dermal photo-protection using a lipoid colloidal carrier. *J. Photochem. Photobiol., B* **2017**, *170*, 49−57.
(35) Bruner, S. D.; Norman, D. P.; Verdine, G. L. Structural basis for recognition and repair of the endogenous mutagen 8-oxoguanine in DNA. *Nature* **2000**, *403*, 859−866.
(36) Vicentini, F. T.; He, T.; Shao, Y.; Fonseca, M. J.; Verri, W. A., Jr; Fisher, G. J.; Xu, Y. Quercetin inhibits UV irradiation-induced inflammatory cytokine production in primary human keratinocytes by suppressing NF-κB pathway. *J. Dermatol. Sci.* **2011**, *61*, 162−168.
(37) Wei, A.; Shibamoto, T. Antioxidant activities and volatile constituents of various essential oils. *J. Agric. Food. Chem.* **2007**, *55*, 1737−1742.
(38) S Jabir, M.; Taha, A. A.; Sahib, U. I. Antioxidant activity of Linalool. *Eng. Technol. J.* **2018**, *36*, 64−67.
(39) Mohebitabar, S.; Shirazi, M.; Bioos, S.; Rahimi, R.; Malekshahi, F.; Nejatbakhsh, F. Therapeutic efficacy of rose oil: A comprehensive review of clinical evidence. *Avicenna J. Phytomed.* **2017**, *7*, 206.
(40) de Cássia da Silveira e Sá, R.; Andrade, L. N.; de Sousa, D. P. A review on anti-inflammatory activity of monoterpenes. *Molecules* **2013**, *18*, 1227−1254.
(41) Lucia Appleton, S.; Navarro-Orcajada, S.; Martínez-Navarro, F. J.; Caldera, F.; López-Nicolás, J. M.; Trotta, F.; Matencio, A. Cyclodextrins as anti-inflammatory agents: basis, drugs and perspectives. *Biomolecules* **2021**, *11* (9), 1384.
(42) González-Ramírez, A. E.; González-Trujano, M. E.; Orozco-Suárez, S. A.; Alvarado-Vásquez, N.; López-Muñoz, F. J. Nerol alleviates pathologic markers in the oxazolone-induced colitis model. *Eur. J. Pharmacol.* **2016**, *776*, 81−89.
(43) Boukani, P. H.; Farahpour, M. R.; Hamishehkar, H. A novel multifaceted approach for infected wound healing: Optimization and in vivo evaluation of Phenethyl alcohol loaded nanoliposomes hydrogel. *J. Drug Delivery Sci. Technol.* **2022**, *77*, No. 103888.
(44) Ganceviciene, R.; Liakou, A. I.; Theodoridis, A.; Makrantonaki, E.; Zouboulis, C. C. Skin anti-aging strategies. *Derm.-Endocrinol.* **2012**, *4*, 308−319.
(45) Tsukahara, K.; Nakagawa, H.; Moriwaki, S.; Takema, Y.; Fujimura, T.; Imokawa, G. Inhibition of ultraviolet-B-induced wrinkle formation by an elastase-inhibiting herbal extract: implication for the mechanism underlying elastase-associated wrinkles. *Int. J. Dermatol.* **2006**, *45*, 460−468.
(46) Imokawa, G. Epithelial−mesenchymal interaction mechanisms leading to the over-expression of neprilysin are involved in the UVB-induced formation of wrinkles in the skin. *Exp. Dermatol.* **2016**, *25*, 2−13.
(47) Imokawa, G.; Ishida, K. Biological mechanisms underlying the ultraviolet radiation-induced formation of skin wrinkling and sagging I: Reduced skin elasticity, highly associated with enhanced dermal elastase activity, triggers wrinkling and sagging. *Int. J. Mol. Sci.* **2015**, *16*, 7753−7775.
(48) Dewi, D. Y. S.; Ginting, C. N.; Chiuman, L.; Girsang, E.; Handayani, R. A. S.; Widowati, W. Potentials of rose (*Rosa damascena*) petals and receptacles extract as antioxidant and antihyaluronidase. *Pharmaciana* **2020**, *10*, 343−352.
(49) Abbas, H.; Sayed, N. S. E.; Youssef, N. A. H. A.; M E Gaafar, P.; Mousa, M. R.; Fayez, A. M.; Elsheikh, M. A. Novel Luteolin-Loaded Chitosan Decorated Nanoparticles for Brain-Targeting Delivery in a Sporadic Alzheimer's Disease Mouse Model: Focus on Antioxidant, Anti-Inflammatory, and Amyloidogenic Pathways. *Pharmaceutics* **2022**, *14*, 1003.
(50) Vergne-Salle, P.; Léger, D. Y.; Bertin, P.; Trèves, R.; Beneytout, J.-L.; Liagre, B. Effects of the active metabolite of leflunomide, A77 1726, on cytokine release and the MAPK signalling pathway in human rheumatoid arthritis synoviocytes. *Cytokine* **2005**, *31*, 335−348.
(51) Saklatvala, J. The p38 MAP kinase pathway as a therapeutic target in inflammatory disease. *Curr. Opin. Pharmacol.* **2004**, *4*, 372−377.
(52) de Launay, D.; van de Sande, M. G.; de Hair, M. J.; Grabiec, A. M.; van de Sande, G. P.; Lehmann, K. A.; Wijbrandts, C. A.; van Baarsen, L. G.; Gerlag, D. M.; Tak, P. P.; Reedquist, K. A. Selective

involvement of ERK and JNK mitogen-activated protein kinases in early rheumatoid arthritis (1987 ACR criteria compared to 2010 ACR/EULAR criteria): a prospective study aimed at identification of diagnostic and prognostic biomarkers as well as therapeutic targets. *Ann. Rheum. Dis.* **2012**, *71*, 415−423.

https://doi.org/10.1021/acsomega.3c04756
ACS Omega 2023, 8, 33943−33954